The Meteoritical Society

Meteoritics & Planetary Science 44, Nr 12, 1937–1946 (2009)
Abstract available online at http://meteoritics.org

Asteroid photometric and polarimetric phase curves: Joint linear-exponential modeling

K. MUINONEN[1, 2], A. PENTTILÄ[1], A. CELLINO[3], I. N. BELSKAYA[4], M. DELBÒ[5], A. C. LEVASSEUR-REGOURD[6], and E. F. TEDESCO[7]

[1]University of Helsinki, Observatory, Kopernikuksentie 1, P.O. BOX 14, FI-00014 U. Helsinki, Finland
[2]Finnish Geodetic Institute, Geodeetinrinne 2, P.O. Box 15, FI-02431 Masala, Finland
[3]INAF-Osservatorio Astronomico di Torino, strada Osservatorio 20, 10025 Pino Torinese, Italy
[4]Astronomical Institute of Kharkiv National University, 35 Sumska Street, 61035 Kharkiv, Ukraine
[5]IUMR 6202 Laboratoire Cassiopée, Observatoire de la Côte d'Azur, BP 4229, 06304 Nice, Cedex 4, France
[6]UPMC Univ. Paris 06, UMR 7620, BP3, 91371 Verrières, France
[7]Planetary Science Institute, 1700 E. Ft. Lowell Road, Tucson, Arizona 85719, USA
*Corresponding author. E-mail: muinonen@cc.helsinki.fi

(Received 01 April, 2009; revision accepted 18 August 2009)

Abstract–We present Markov-Chain Monte-Carlo methods (MCMC) for the derivation of empirical model parameters for photometric and polarimetric phase curves of asteroids. Here we model the two phase curves jointly at phase angles $\leqslant 25°$ using a linear-exponential model, accounting for the opposition effect in disk-integrated brightness and the negative branch in the degree of linear polarization. We apply the MCMC methods to V-band phase curves of asteroids 419 Aurelia (taxonomic class F), 24 Themis (C), 1 Ceres (G), 20 Massalia (S), 55 Pandora (M), and 64 Angelina (E). We show that the photometric and polarimetric phase curves can be described using a common nonlinear parameter for the angular widths of the opposition effect and negative-polarization branch, thus supporting the hypothesis of common physical mechanisms being responsible for the phenomena. Furthermore, incorporating polarimetric observations removes the indeterminacy of the opposition effect for 1 Ceres. We unveil a trend in the interrelation between the enhancement factor of the opposition effect and the angular width: the enhancement factor decreases with decreasing angular width. The minimum polarization and the polarimetric slope at the inversion angle show systematic trends when plotted against the angular width and the normalized photometric slope parameter. Our new approach allows improved analyses of possible similarities and differences among asteroidal surfaces.

INTRODUCTION

Two ubiquitous phenomena are observed for asteroids and other atmosphereless solar system objects as well as for cometary and interplanetary dust near opposition: a negative branch in the degree of linear polarization ("negative polarization") and a nonlinear enhancement of brightness (opposition effect). Negative polarization refers to the case where the scattered intensity component parallel to the Sun-object-observer plane (scattering plane) predominates over the one perpendicular to the plane. The negative-polarization and opposition-effect phenomena are constrained to Sun-object-observer angles (phase angles) of $\leqslant 25°$ and $\leqslant 10°$, respectively. In some cases, the phenomena show up at extremely small phase angles within a degree from opposition (Harris et al. 1989b; Rosenbush 2009), whereas in some cases negative polarization, in particular, extends over a wide range in phase angle (Cellino et al. 2006).

Coherent backscattering, single scattering, and shadowing have been considered as mechanisms responsible for the phenomena (see review in Muinonen et al. 2002a). Coherent backscattering is an interference mechanism that can contribute to both brightness and polarization (Hapke 1990; Muinonen 1989, 1990; Shkuratov 1985, 1988, 1989; Mishchenko and Dlugach 1993), single-scattering interference effects can contribute to both phenomena over a wider range of phase angles (e.g., Muinonen et al. 2007; Tyynelä et al. 2007) whereas shadowing is thought to contribute to the opposition effect only (see Muinonen et al. 2002a).

We analyze the photometric and polarimetric phase curves jointly by using an empirical model developed to fit the observations within the observational errors given. Empirical models are useful in planning further observations of the objects and in grouping the objects based on the similarities and differences in their phase curves. Note the important role played by the *H*, *G* magnitude system (Bowell et al. 1989) for asteroid research at large, and the ongoing efforts to improve the system (Muinonen et al. 2008).

The present study emerges from the earlier ones for estimating the parameters of the brightness opposition effect (e.g., Bowell et al. 1989; Lumme et al. 1993; Belskaya and Shevchenko 2000; Muinonen et al. 2002b; Rosenbush et al. 2002; Kaasalainen et al. 2003; Avramchuk et al. 2007) and of the negative polarization (e.g., Muinonen et al. 2002b; Rosenbush et al. 2002; Kaasalainen et al. 2003; Lumme and Muinonen 2003; Levasseur-Regourd 2003, 2004). We seek answers to the question whether it is possible to explain the photometric and polarimetric phase curves with a joint empirical model involving common parameters for photometry and polarimetry. Here we present the results of studies at phase angles $\leqslant 25°$. We provide practical Markov-Chain Monte-Carlo methods (MCMC) for obtaining reliable error estimates for nonlinear model parameters. Note that Penttilä et al. (2005) made use of MCMC methods in their statistical analyses of asteroidal and cometary polarization phase curves using the trigonometric (Lumme and Muinonen 2003) and polynomial models (Levasseur-Regourd 2004).

In the Theoretical and Numerical Methods section, we summarize the linear-exponential model for the photometric and polarimetric applications and describe the MCMC methods for sampling the parameters. Section 3 includes the application of the methods to the V-band photometric and polarimetric phase curves of asteroids 419 Aurelia (taxonomic class F), 24 Themis (C), 1 Ceres (G), 20 Massalia (S), 55 Pandora (M), and 64 Angelina (E). We close the paper with conclusions and future prospects.

THEORETICAL AND NUMERICAL METHODS

Linear-Exponential Modeling

We start with the four-parameter empirical linear-exponential model for the photometric and polarimetric phase curves close to the opposition (Muinonen et al. 2002b; Kaasalainen et al. 2003):

$$f(\alpha) = a \exp\left(-\frac{\alpha}{d}\right) + b + k\alpha, \tag{1}$$

where α is the phase angle, a, b, and k are the three linear parameters, and d is the single nonlinear parameter. Note that the linear-exponential model does not describe polarimetric and photometric phase curves at phase angles >30°: the polarimetric phase curves show maxima near 90° and the photometric phase curves must be constrained to positive values at all phase angles. Nevertheless, the linear-exponential model is suitable for the present study at small phase angles.

In order to distinguish between the photometric and polarimetric parameters, subscripts I (for intensity) and P (for polarization) are attached to the symbols a, b, k, and d. For photometry, the empirical parameters are the amplitude a_I and angular width d_I of the opposition effect, the background brightness b_I, and the slope k_I. By normalization at zero phase angle, the number of parameters decreases to three. For polarimetry, the empirical parameters are the amplitude a_P and angular width d_P of the negative-polarization branch, the balancing amplitude b_P, and the slope k_P. Based on the physics of light scattering, we assume $b_P = a_P$ so that the degree of linear polarization is zero at zero phase angle. For the joint linear-exponential modeling, we assume $d = d_I = d_P$ so that d is the single common nonlinear parameter in the interpretation of the photometric and polarimetric phase curves.

There are additional dependent parameters that are of interest in comparative studies. For the opposition effect, such parameters are, e.g., the enhancement factor ζ and the angular half-width at half-maximum $d_{\frac{1}{2}I}$,

$$\zeta = \frac{a_I + b_I}{b_I},$$

$$d_{\frac{1}{2}I} = d_I \ln 2. \tag{2}$$

For the negative polarization branch, the phase angle $\alpha_{\min}$ and value of minimum polarization $P_{\min}$ are of special interest:

$$\alpha_{\min} = -d_P \ln\left(\frac{k_P d_P}{a_P}\right),$$

$$P_{\min} = k_P d_P \left[1 - \ln\left(\frac{k_P d_P}{a_P}\right)\right] + b_P. \tag{3}$$

The inversion angle of polarization α_0 needs to be solved from an implicit equation (using, e.g., Newton's method):

$$a_P \exp\left(-\frac{\alpha_0}{d_P}\right) + b_P + k_P \alpha_0 = 0. \tag{4}$$

The corresponding first derivative P_0' gives the slope of the polarization curve at the inversion angle which is known to correlate with the geometric albedo and is used to derive reliable diameter estimates (see Cellino et al. 1999 and, in particular, Belskaya et al. 2009 for wavelength dependences):

$$P_0' = \frac{b_P + k_P \alpha_0 + k_P d_P}{d_P}. \tag{5}$$

Markov-Chain Monte-Carlo Methods

The photometric and polarimetric phase curves are analyzed using techniques developed further from those in Muinonen et al. (2002b) and Kaasalainen et al. (2003). The a posteriori probability density function (p.d.f.) for the parameters $\boldsymbol{P} = (a, d, b, k)$ (for models separate for photometry and polarimetry) is obtained from

$$p(\boldsymbol{P}) \propto \exp\left[-\frac{1}{2}\chi^2(\boldsymbol{P})\right], \quad (6)$$

where χ^2 denotes the square form composed of the matrix product of the O-C residuals (observed minus computed) and the covariance matrix for the random observational errors. In what follows, for simplicity, the covariance matrix is assumed to be diagonal.

In earlier works (Muinonen et al. 2002b; Kaasalainen et al. 2003), we have additionally included Jeffreys' a priori p.d.f. (Jeffreys 1948) as a multiplying p.d.f. on the right-hand side of Equation 6. Jeffreys' p.d.f is, in essence, a Jacobian which guarantees that the probabilistic interpretation is invariant in transformations from one nonlinear parameter set to another. We omit Jeffreys' p.d.f. due to two main reasons: first, it would introduce an additional indirect dependence on the observations; second, it would render the modeling disproportionately complicated for the present study.

We sample the a posteriori p.d.f. $p(\boldsymbol{P})$ in Equation 6 using the classical Metropolis-Hastings MCMC method (Gilks et al. 1996). For the so-called proposal p.d.f. $q(\boldsymbol{P}, \boldsymbol{P}_j)$ centered at $\boldsymbol{P}_j$ with the proposed new value $\boldsymbol{P}$, a new set of parameters is accepted as $\boldsymbol{P}_{j+1} = \boldsymbol{P}$ if, for a random deviate $y \in [0,1]$,

$$y < \frac{p(\boldsymbol{P})q(\boldsymbol{P}, \boldsymbol{P}_j)}{p(\boldsymbol{P}_j)q(\boldsymbol{P}_j, \boldsymbol{P})}. \quad (7)$$

Otherwise $\boldsymbol{P}_{j+1} = \boldsymbol{P}_j$. If q is symmetric, the acceptance criterion reduces to

$$y < \frac{p(\boldsymbol{P})}{p(\boldsymbol{P}_j)}. \quad (8)$$

In the present study, we utilize symmetric univariate Gaussian proposal p.d.f.'s for each of the elements in $q(\boldsymbol{P}, \boldsymbol{P}_j)$. It can be shown that, under quite general conditions, the chain $\boldsymbol{P}_1, \boldsymbol{P}_2, \boldsymbol{P}_3, \ldots$ approaches to sample from the correct distribution for $\boldsymbol{P}$.

For the joint empirical modeling, the six free parameters are $\boldsymbol{P} = (d, a_I, b_I, k_I, a_P, k_P)$ and, following the assumption of Gaussian observational errors, we define

$$\chi^2 = \chi^2_I + \chi^2_P, \quad (9)$$

where χ^2_I and χ^2_P are the χ^2 values of the photometric and polarimetric fits, respectively, with the two data sets taken to have uncorrelated observational errors.

RESULTS AND DISCUSSION

The photometric and polarimetric phase curves of asteroids 419 Aurelia (class F), 24 Themis (C), 1 Ceres (G), 20 Massalia (S), 55 Pandora (M), and 64 Angelina (E) in the V band are shown in Figs. 1 and 2, respectively, with the corresponding references and additional information on the observations summarized in Table 1. We have chosen these asteroids for the present study because their phase curves are representative of the types of phase curves observed for asteroids. Note, however, that there are still only small numbers of asteroids with sufficient phase-curve coverage in both photometry and polarimetry.

For the individual photometric phase curves, all the error standard deviations of the magnitude points are assumed to be the same; and, for the individual polarimetric phase curves, all the error standard deviations of the polarization points are assumed to be the same. The error standard deviations are determined as follows. For each individual photometric phase curve, a best-fit four-parameter linear-exponential model is derived using equal weights for the observations. The rms value of the fit is then chosen to be the error standard deviation for all the observations of that specific phase curve. An analogous procedure is carried out for each polarimetric phase curve. We have followed this choice because of either missing detailed information on the errors (for photometry) or somewhat inhomogeneous error estimates (for polarimetry) and stress that the main conclusions of the study are not affected by the choice of the error model.

In Figs. 1 and 2, we show the 3σ or 99.7% error envelopes as obtained via MCMC with 50000 differing parameter sets (with varying numbers of repetitions for each set) in a joint treatment of photometry and polarimetry. At any given phase angle, the envelope is constructed from the minimum and maximum values as given by the sample model parameters belonging to the 3σ regime of the parameters. Outside the phase-angle ranges covered by the observations but still within the phase-angle range of applicability for the linear-exponential model, the best-fit models and the envelopes serve as realistic predictors for the photometric and polarimetric phase curves, although the purely empirical character of the models limits their predictive value.

The MCMC method works efficiently in the joint treatment of photometry and polarimetry, with a delivery of 50000 samples within a few CPU seconds on a modern personal computer. This is a remarkable improvement in speed as compared to the earlier p.d.f. characterizations for the linear-exponential model separately for photometry and polarimetry (e.g., Muinonen et al. 2002b; Kaasalainen et al. 2003). However, when comparing the computational speed to that of the earlier work, it is important to bear in mind that Jeffreys' a priori p.d.f. (Jeffreys 1943), excluded currently but included earlier, commonly introduces a computational burden. Note that the so-called burn-in phase in MCMC

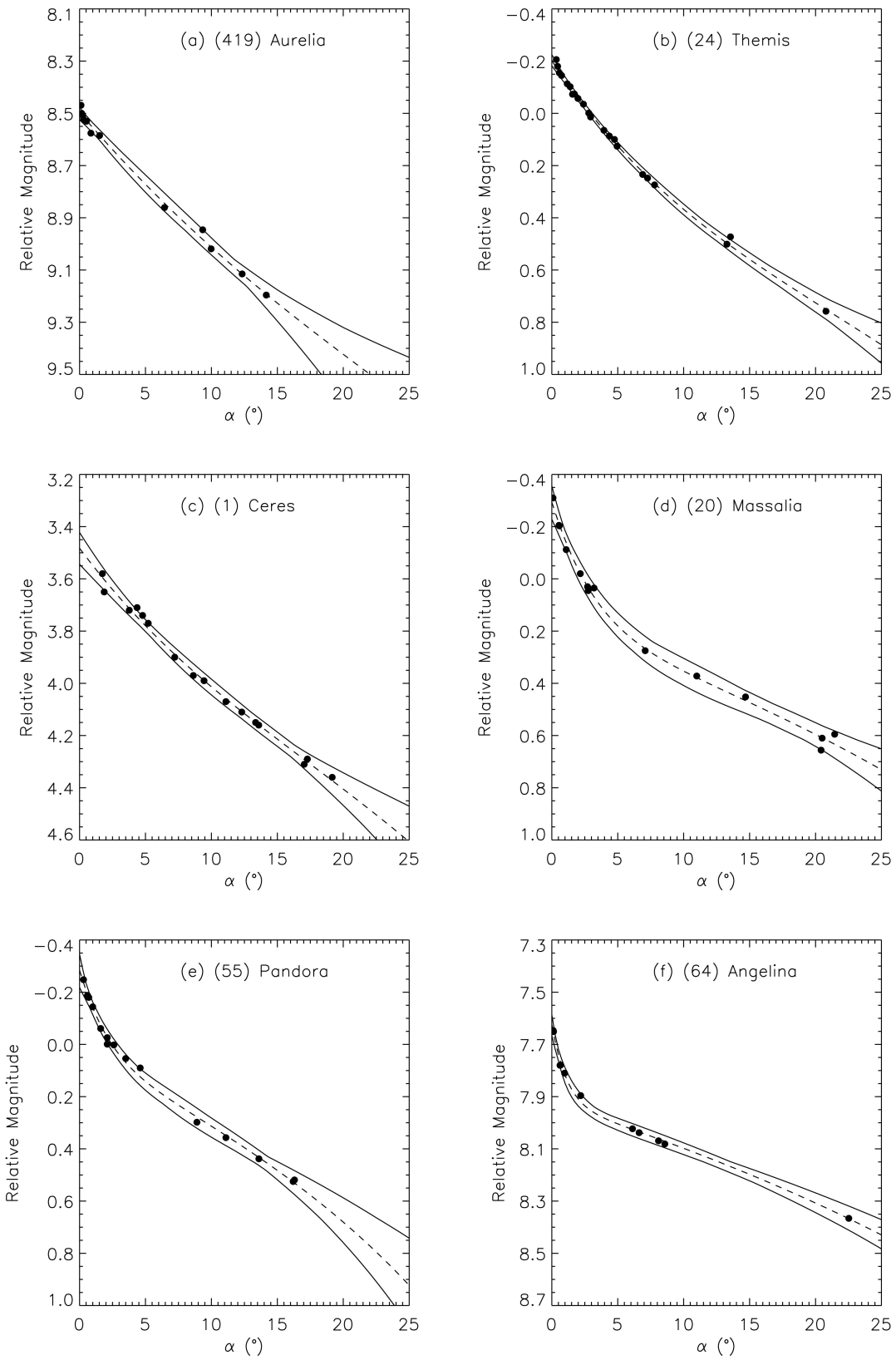

Fig. 1. Best-fit linear-exponential models (dashed lines) with MCMC-based 3σ (99.7%) error envelopes (solid lines) for the photometric observations of the following asteroids: a) 419 Aurelia (taxonomic class F), b) 24 Themis (C), c) 1 Ceres (G), d) 20 Massalia (S), e) 55 Pandora (M), and f) 64 Angelina (E). See Table 1 for additional information on and references to the observations.

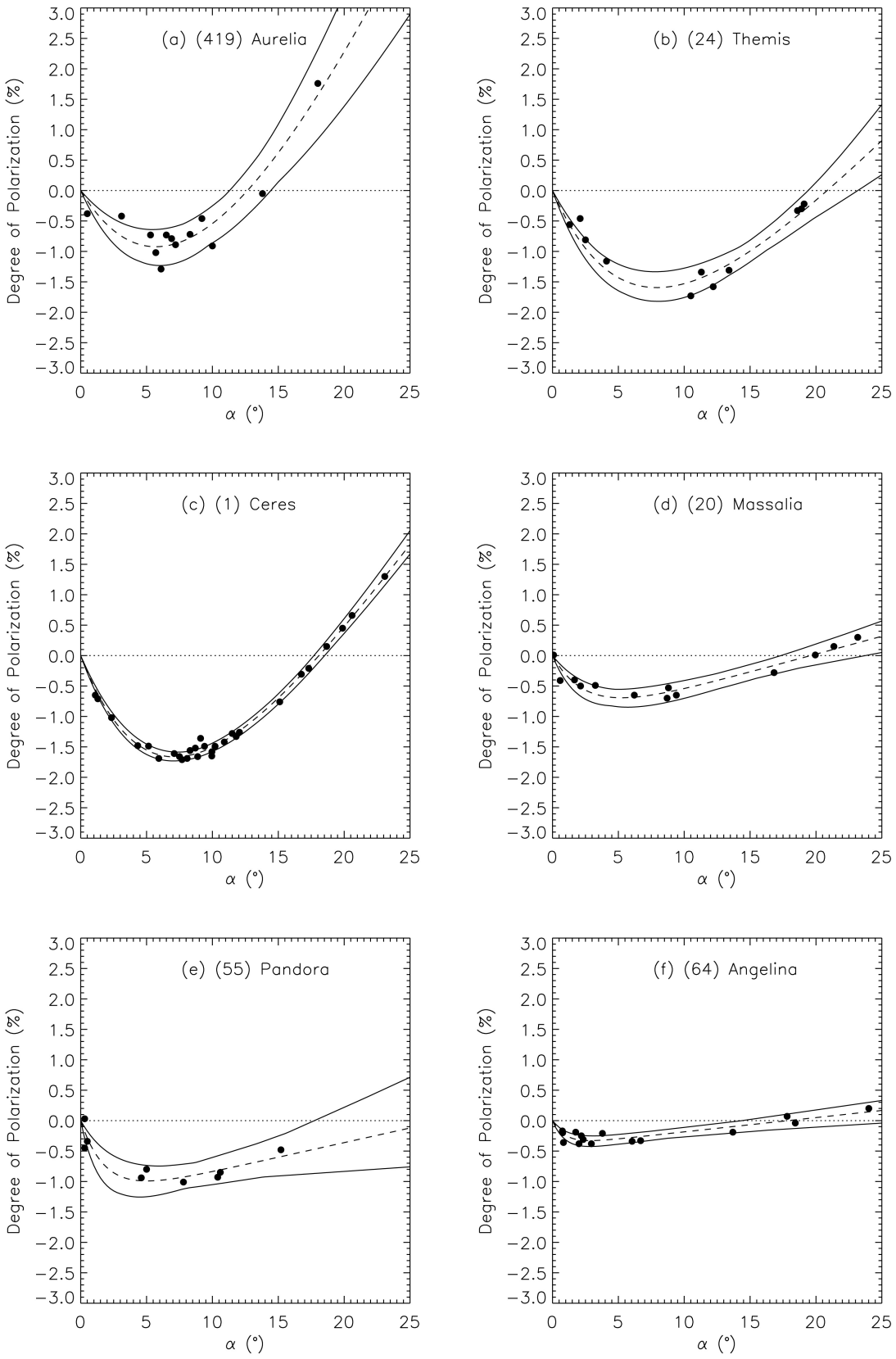

Fig. 2. As in Fig. 1 for the polarimetric observations.

Table 1. Asteroids utilized in the joint linear-exponential modeling of the photometric (label *I*) and polarimetric phase curves (*P*). We show the number of observations N_{obs}, the minimum and maximum phase angles of the observations $\alpha<$ and $\alpha>$ (°), the error standard deviations σ_{fit} for the photometric (in mag) and polarimetric observations (in %) and the references to the observations.

	Asteroid	N_{obs}	$\alpha<$	$\alpha>$	σ_{fit}	References
I	419 Aurelia	13	0.11	14.2	0.014	Belskaya et al. 2002
	24 Themis	22	0.34	20.8	0.010	Harris et al. 1989a
	1 Ceres	16	1.73	19.2	0.018	Tedesco et al. 1983
	20 Massalia	14	0.09	21.4	0.023	Gehrels 1956; Belskaya et al. 2003
	55 Pandora	15	0.3	16.3	0.015	Shevchenko et al. 1993
	64 Angelina	11	0.11	22.5	0.011	Harris et al. 1989a
P	419 Aurelia	13	0.5	18.0	0.21	Belskaya et al. 2005
	24 Themis	11	1.3	19.1	0.11	Chernova et al. 1994
	1 Ceres	29	1.11	23.1	0.071	Zellner et al. 1974; Zellner and Gradie 1976
	20 Massalia	13	0.08	23.2	0.089	Belskaya et al. 2003; Zellner and Gradie 1976
	55 Pandora	9	0.3	15.2	0.14	Lupishko et al. 1994
	64 Angelina	18	0.75	18.4	0.071	Zellner and Gradie 1976; Rosenbush et al. 2005

Table 2. Parameters of joint linear-exponential photometric and polarimetric models for the asteroids in Table 1 with MCMC-based two-sided error estimates that give the minimum and maximum deviations of each parameter within the top 3σ or 99.7% fraction of parameter sets sampled. We show the rms-values of the photometric and polarimetric fits, angular width *d*, normalized opposition-effect amplitude a_I/b_I (the enhancement factor $\zeta = 1 + a_I/b_1$), normalized photometric slope k_I/b_I, polarimetric amplitude a_P, and the polarimetric slope k_P.

	419 Aurelia	24 Themis	1 Ceres	20 Massalia	55 Pandora	64 Angelina
rms (mag)	0.017	0.012	0.019	0.023	0.015	0.011
rms (%)	0.24	0.17	0.071	0.095	0.15	0.072
d (°)	10.5	6.71	6.77	2.59	1.87	1.00
	–4.4	–2.0	–0.48	–0.69	–0.72	–0.28
	+5.7	+2.2	+1.46	+1.22	+1.48	+0.48
a_I/b_I	0.94	0.68	0.51	0.55	0.352	0.317
	–0.44	–0.22	–0.20	–0.13	–0.083	–0.055
	+0.06	+0.32	+0.34	+0.22	+0.141	+0.054
k_I/b_I ((°)$^{-1}$)	–0.0157	–0.0160	–0.0191	–0.0159	–0.0222	–0.0149
	–0.0120	–0.0038	–0.0040	–0.0030	–0.0031	–0.0017
	+0.0061	+0.0059	+0.0069	+0.0042	+0.0052	+0.0018
a_P (%)	8.92	4.84	5.86	1.15	1.32	0.42
	–4.3	–1.4	–0.26	–0.26	–0.40	–0.11
	+8.3	+2.1	+1.08	+0.45	+0.56	+0.13
k_P (%(°)$^{-1}$)	0.49	0.222	0.3016	0.059	0.048	0.023
	–0.17	–0.072	–0.0091	–0.018	–0.037	–0.012
	+0.28	+0.095	+0.0418	+0.026	+0.052	+0.010

sampling, the computational phase where the Markov chain approaches the regime of higher p.d.f. values, is here absent since the chains are initiated with parameter values already resulting in good fits to the observations.

Table 2 shows the rms-values of the photometric and polarimetric fits. Comparing the rms-values to the assumed standard deviations of the observational errors tabulated in Table 1 shows a modest deterioration of the fits for a number of objects when the photometric and polarimetric observations are treated jointly. This is the price we are paying for reducing the number of parameters and using a simple empirical model instead of a physical or more evolved empirical model. A study of the statistical significance of the deterioration is left for future. We only note that the rms values of the fits using the joint model are in accordance with the overall variation among the data points for each asteroid.

Also shown in Table 2 are the best-fit model parameters together with their two-sided error estimates based on the maximum extent of each parameter within the 3σ regime. For an example of MCMC sampling, for asteroid 1 Ceres, the standard deviations of the Gaussian proposal p.d.f.'s for *d*, a_I, b_I, k_I, a_P, and k_P are 0.03°, 0.003, 0.0001, 0.000007(°)$^{-1}$, 0.03, and 0.0002(°)$^{-1}$, respectively. The full Markov chain consists of 222688 entries, resulting in the required 50000 different samples and an efficiency of 22%. Note that a purely photometric modeling of 1 Ceres would result in complete indeterminacy insofar as the angular width of the opposition effect is concerned. The indeterminacy is removed by the

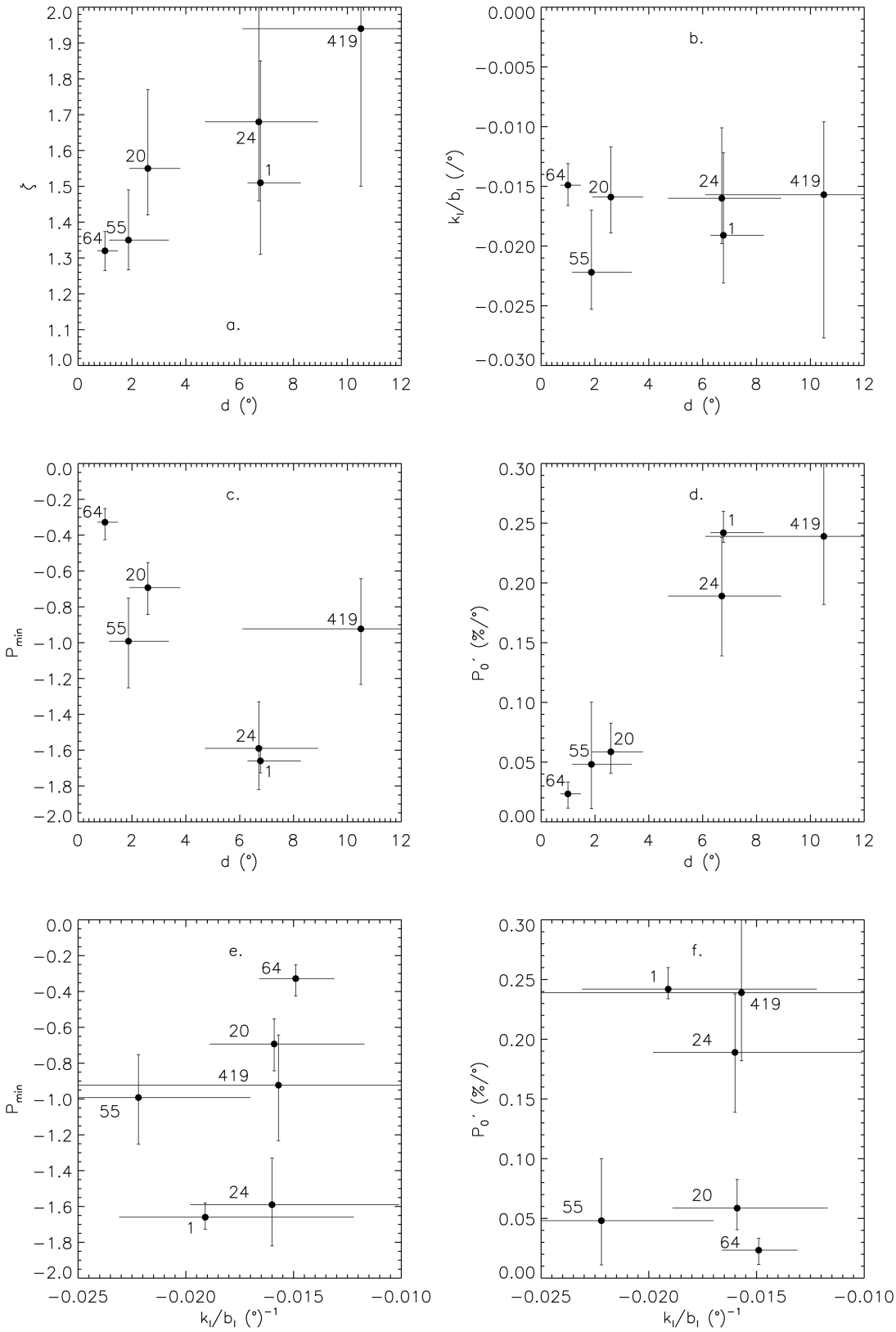

Fig. 3. Opposition-effect and negative-polarization parameters against the angular width d for the six asteroids studied (Table 1): a. enhancement factor ζ, b. normalized photometric slope k_l/b_l, c. minimum polarization $P_{\min}$, and d. polarimetric slope P'_0. Also shown are parameters against the normalized photometric slope k_l/b_l: e. $P_{\min}$ and f. P'_0.

Table 3. As in Table 2 for the phase angle of minimum polarization min, minimum polarization $P\alpha_{min}$, inversion angle of polarization α_0, and the polarimetric slope at the inversion angle P'_0.

	419 Aurelia	24 Themis	1 Ceres	20 Massalia	55 Pandora	64 Angelina
α_{min} (°)	5.70	7.91	7.19	5.24	5.0	2.88
	–0.70	–0.77	–0.30	–0.83	–1.5	–0.62
	+0.95	+0.80	+0.42	+1.21	+2.5	+0.93
P_{min} (%)	–0.92	–1.59	–1.66	–0.69	–0.99	–0.328
	–0.31	–0.23	–0.067	–0.15	–0.26	–0.097
	+0.28	+0.26	+0.079	+0.14	+0.24	+0.077
α_0 (°)	12.7	20.8	18.10	19.6	27.5	17.9
	–1.4	–1.4	–0.38	–2.3	–9.8	–3.5
	+1.8	+2.3	+0.43	+4.1	+6.5	+10.3
P'_0 (%(°)$^{-1}$)	0.239	0.189	0.2417	0.059	0.048	0.023
	–0.057	–0.050	–0.0081	–0.018	–0.037	–0.012
	+0.063	+0.048	+0.0178	+0.024	+0.052	+0.010

joint treatment of the photometric and polarimetric data sets. In the final Table 3, we show α_{min}, P_{min}, α_0, and P'_0 with their error estimates.

Figure 3 shows the enhancement factors ζ versus angular widths d with the error bars (as described above and included in Table 2) for the six asteroids. First, for 419 Aurelia with an almost linear phase curve, the distribution is wide as can be expected. Second, the points for 24 Themis and 1 Ceres are next to one another in agreement with potential similarities in the composition of the asteroids. Note that 1 Ceres is unusual among G-class asteroids: it has a slightly smaller inversion angle than other G-class asteroids observed (Goidet-Devel et al. 1995). Third, the domain of 55 Pandora is overlapping, on one hand, with the domain of 64 Angelina and, on the other hand, with the domain of 20 Massalia. There could be compositional reasons for a similar opposition effect for these objects: Rivkin et al. (2000) have confirmed hydrated minerals on the surface of 55 Pandora and placed 55 Pandora in a separate taxonomic class W instead of M. Further studies are needed but are beyond the scope of the present study. A systematic trend appears to result, spanning from the low-albedo to high-albedo asteroids (the albedo being here the geometric albedo).

We plot k_I/b_I versus d (Fig. 3b), P_{min} versus d (Fig. 3c), and P'_0 versus d (Fig. 3d) for the same asteroids. Whereas k_I/b_I versus d shows no clear trends, P_{min} versus d and P'_0 versus d show almost linear trends of deepening P_{min} and steepening polarimetric slope with increasing d. The F-class asteroid 419 Aurelia appears to provide an intriguing exception to the linear trend in P_{min} versus d. Last but not least, there are hints about a bimodal structure of the patterns, with none of the present asteroids showing angular widths around 4–4.5°. The polarimetric parameters of 55 Pandora lie close to those of 20 Massalia, with P_{min} distinguishing 55 Pandora from 64 Angelina.

We further plot P_{min} versus k_I/b_I (Fig. 3e) and P'_0 versus k_I/b_I (Fig. 3f). Within the errors depicted, we can envisage a trend for P_{min} versus k_I/b_I as reported by Shevchenko (1997) and a trend for P'_0 versus k_I/b_I. For these two trends to be real, the true value for the photometric slope of 419 Aurelia should be located towards the left in the corresponding error domain and that the true value for the slope of 55 Pandora should be located towards the right in the error domain. Further confirmation would require more polarimetric data on these asteroids.

CONCLUSION

We have succeeded in fitting the representative photometric and polarimetric phase curves for six asteroids of differing taxonomic classes using a joint linear-exponential model with the angular width of the opposition effect and the negative-polarization branch as the common parameter. It has not been a priori certain that the method would work. We conclude that it is probable that common physical mechanisms are responsible for the phenomena and that the present study encourages the development of joint physical models for the phase curves. We stress the importance of acquiring additional photometric and polarimetric observations of asteroids to extend the present analysis to increasing numbers of objects.

MCMC methods provide high performance in both separate and joint empirical modeling of the photometric and polarimetric phase curves of asteroids. Error estimates follow rapidly and rigorously for both linear and nonlinear parameters. We envisage application of MCMC to the phase curves of additional asteroids as well as comets.

Acknowledgments–The authors express their gratitude to ISSI for making their collaboration possible as an ISSI International Team. K. M.'s research has been partially supported by the EU/TMR project entitled "European Leadership in Space Astrometry" (ELSA). A. C. acknowledges ASI (Contract no. I/015/07/0) for enabling his work in Bern. M. D. carried out part of the research while he was Henri Poincare' Fellow at the Observatoire de la Cote d'Azur. The Henri Poincare' Fellowship is funded by the CNRS-INSU, the Conseil General des Alpes-Maritimes and the Rotary International—District 1730. A. C. L. R. acknowledges partial funding from CNES. E. T.'s participation in this effort was supported through NASA

Subcontract no. 132416 under NASA JPL prime contract task order no. NMO7108563.

Editorial Handling—Dr. Nancy Chabot

REFERENCES

Avramchuk V. V., Rosenbush V. K., and Bul'Ba T. P. 2007. Photometric study of the major satellites of Uranus. *Solar System Research* 41:186–202.

Belskaya I. N. and Shevchenko V. G. 2000. Opposition effect of asteroids. *Icarus* 147:94–105.

Belskaya I. N., Shevchenko V. G., Efimov Yu. S., Shakhovskoy N. M., Shkuratov Yu. G., Gaftonyuk N. M., Gil-Hutton R., Krugly Yu. N., and Chiorny V. G. 2002. Opposition polarimetry and photometry of the low albedo asteroid 419 Aurelia. In *Proceedings of Asteroids, Comets, Meteors 2002*. Berlin: ESA Publishing Division. pp. 489–491.

Belskaya I. N., Shevchenko V. G., Kiselev N. N., Krugly Yu., N., Shakhovskoy N. M., Efimov Yu. S., Gaftonyuk N. M., Cellino A., and Gil-Hutton R. 2003. Opposition polarimetry and photometry of S and E-type asteroids. *Icarus* 166:276–284.

Belskaya I. N., Shkuratov Yu. G., Emov Yu. S., Shakhovskoy N. M., Gil-Hutton R., Cellino A., Zubko E. S., Ovcharenko A. A., Bondarenko S. Yu., Shevchenko V. G., Fornasier S., Barbieri C. 2005. The F-type asteroids with small inversion angles of polarization. *Icarus* 178:213–221.

Belskaya I. N., Levasseur-Regourd A. C., Cellino A., Emov Y. S., Shakhovskoy N. M., Hadamcik E., and Bendjoya P. 2009. Polarimetry of main belt asteroids: Wavelength dependence. *Icarus* 199:97–105.

Bowell E., Hapke B., Lumme K., Harris A. W., Domingue D., and Peltoniemi J. I. 1989. Application of Photometric Models to Asteroids, in *Asteroids II*, edited by Binzel R. P., Gehrels T., and Matthews M. Tucson: The University of Arizona Press. pp. 524–556.

Cellino A., Gil Hutton R., Tedesco E. F., Di Martino M., and Brunini A. 1999. Polarimetric observations of small asteroids: preliminary results. *Icarus* 138:129–140.

Cellino A., Belskaya I. N., Bendjoya P., Di Martino M., Gil-Hutton R., Muinonen K., and Tedesco E. F. 2006. The strange polarimetric behavior of asteroid (234) Barbara. *Icarus* 180:565–567.

Chernova G. P., Lupishko D. F., and Shevchenko V. G. 1994. Photometry and polarimetry of asteroid 24 Themis. *Kinemat. Phys. Neb. Tel.* 10(2):45–49.

Gehrels T. 1956. Photometric studies of asteroids: V. The lightcurve and phase function of 20 Massalia. *The Astronomical Journal* 123:331–335.

Gilks W. R., Richardson S., and Spiegelhalter D. J. 1996. Markov Chain Monte Carlo in practice. Chapman and Hall/CRC.

Goidet-Devel B., Renard J. B., and Levasseur-Regourd A. C. 1995. Polarization of asteroids: Synthetic curves and characteristic parameters. *Planetary and Space Science* 43:779–786.

Hapke B. 1990. Coherent backscatter and the radar characteristics of outer planet satellites. *Icarus* 88:407–417.

Harris A. W., Young J. W., Bowell E., Martin L. J., Millis R. L., Poutanen M., Scaltriti F., Zappalà, V., Schober H. J., Debehogne H., and Zeigler K. W. 1989a. Photoelectric observation of asteroids 3, 24, 60, 261, 863. *Icarus* 77:171–186.

Harris A. W., Young J. W., Contreiras L., Dockweiler T., Belkora L., Salo H., Harris W. D., Bowell E., Poutanen M., Binzel R. P., Tholen D. J., and Wang S. 1989b. Phase relations of high albedo asteroids: The unusual opposition brightening of 44 Nysa and 64 Angelina. *Icarus* 81:365–374.

Jeffreys H. 1946. An invariant form for the prior probability in estimation problems. *Proceedings of the Royal Statistical Society of London*, *Series A* 186:453–461.

Kaasalainen S., Piironen J., Kaasalainen M., Harris A. W., Muinonen K., and Cellino A. 2003. Asteroid photometric and polarimetric phase curves: Empirical interpretation. *Icarus* 161:34–46.

Levasseur-Regourd A. C. 2003. Cosmic dust physical properties. *Advances in Space Research* 31:2599–2606.

Levasseur-Regourd A. C. 2004. Polarimetry of dust in the solar system: Remote observations, in situ measurements and experimental simulations. In *Photopolarimetry in remote sensing*, edited by Videen G., Yatskiv Y., and Mishchenko M. Dordrecht: Kluwer Academic Publishers. 393–410.

Lumme K. and Muinonen K. 1993. A two-parameter system for linear polarization of some solar system objects. Asteroids, Comets, Meteors 1993. IAU Symposium vol. 160. p. 194.

Lumme K., Muinonen K., Harris A. W., and Bowell E. 1993. A new three–parameter magnitude system for asteroids. *Bulletin of the American Astronomical Society* 25:1125.

Lupishko D. F., Kiselev N. N., Chernova G. P., Shakhovskoj N. M., and Vasilyev S. V. 1994. Polarization phase dependences of asteroids 55 Pandora and 704 Interamnia. *Kinemat. Phys. Neb. Tel* 10(2):40–44.

Mishchenko M. I. and Dlugach J. M. 1993. Coherent backscatter and the opposition effect for E-type asteroids. *Planetary and Space Science* 41:173–181.

Muinonen K. 1989. Electromagnetic scattering by two interacting dipoles *Proceedings of the 1989 URSI Electromagnetic Theory Symposium*. pp. 428–430.

Muinonen K. 1990. Light Scattering by Inhomogeneous Media: Backward Enhancement and Reversal of Polarization, Ph.D. thesis, University of Helsinki, Finland.

Muinonen K., Piironen J., Shkuratov Yu. G., Ovcharenko A., and Clark B. E. 2002a. Asteroid photometric and polarimetric phase effects. In *Asteroids III*, edited by Bottke W., Binzel R. P., Cellino A., and Paolicchi P. Tucson: The University of Arizona Press. pp. 123–138.

Muinonen K., Piironen J., Kaasalainen S., and Cellino A. 2002b. Asteroid photometric and polarimetric phase curves: Empirical modeling. *Memorie Della Società Astronomica Italiana—Journal of the Italian Astronomical Society* 73:716–721.

Muinonen K., Zubko E., Tyynelä J., Shkuratov Yu. G., and Videen G. 2007. Light scattering by Gaussian random particles with discrete-dipole approximation. *Journal of Quantitative Spectroscopy and Radiative Transfer* 106:360–377.

Muinonen K., Cellino A., Belskaya I., Delbo M., Levasseur-Regourd A. C., and Tedesco E. F. 2008. Inversion of asteroid phase curves for empirical magnitude and polarization systems. In Asteroids, Comets, Meteors 2008, July 13–18, 2008, Baltimore, Maryland, USA. LPI Contribution 1405. p. 8263.

Penttilä A., Lumme K., Hadamcik E., and Levasseur-Regourd A. C. 2005. Statistical analysis of asteroidal and cometary polarization phase curves. *Astronomy and Astrophysics* 432:1081–1090.

Rivkin A., Howell E. S., Lebofsky L. A., Clark B. E., and Britt D. T. 2000. The nature of M-class asteroids from 3-μm observations. *Icarus* 145:351–368.

Rosenbush V., Kiselev N., Avramchuk V., and Mishchenko M. 2002. Photometric and polarimetric opposition phenomena exhibited by solar system bodies. In *Optics of cosmic dust*, edited by Videen G. and Kocifaj M. NATO Science Series. Dordrecht/Boston/London: Kluwer Academic Publishers. pp. 191–226.

Rosenbush V. K., Kiselev N. N., Shevchenko V. G., Jockers K., Shakhovskoy N. M., and Efimov Yu. S. 2005. Polarization and brightness opposition effects for the E-type asteroid 64 Angelina. *Icarus* 178:222–234.

Rosenbush V. K., Shevchenko V. G., Kiselev N. N., Sergeev

A. V., Shakhovskoy N. M., Velichko F. P., Kolesnikov S. V., and Karpov N. V. 2009. Polarization and brightness opposition effects for the E-type Asteroid 44 Nysa. *Icarus* 201:655–665. Shevchenko V. G., Krugly Yu. N., Lupishko D. F., Harris A. W., and Chernova G. P. 1993. Lightcurves and phase relations of asteroid 55 Pandora. *Astronomicheskii Vestnik* 27(3):75–80.

Shevchenko V. G. 1997. Analysis of asteroid brightness-phase relations. *Solar System Research* 31:219–224.

Shkuratov Yu. G. 1985. On the origin of the opposition effect and negative polarization for cosmic bodies with solid surface. *Astronomical Circular No. 1400*, Sternberg State Astronomy Institute, Moscow. pp. 3–6.

Shkuratov Yu. G. 1988. Diffractional model of the brightness surge of complex structures. *Kin. Phys. Neb. Tel.* 4:60–66.

Shkuratov Yu. G. 1989. A new mechanism of the negative polarization of light scattered by the surfaces of atmosphereless celestial bodies. *Astronomicheskii Vestnik* 23:176–180.

Tedesco E. F., Taylor R. C., Drummond J., Harwood D., Nickoloff I., Scaltriti F., Schober H. J., and Zappalà, V. 1983. Worldwide photometry and lightcurve observations of 1 Ceres during the 1975–1976 apparition. *Icarus* 54:23–29.

Tyynelä J., Zubko E., Videen G., and Muinonen K. 2007. Interrelating angular scattering characteristics to internal electric fields for wavelength-scale spherical particles. *Journal of Quantitative Spectroscopy and Radiative Transfer* 106:520–534.

Zellner B. and Gradie J. 1976. Minor planets and related objects. XX. Polarimetric evidence for the albedos and compositions of 94 asteroids. *The Astronomical Journal* 81:262–280.

Zellner B., Gehrels T., and Gradie J. 1974. Minor planets and related objects. XVI. Polarimetric diameters. *The Astronomical Journal* 79:1100–1110.